Recent results from the HIT-SI experiment

T. R. Jarboe 1), C. Akcay 1), M. A. Chilenski 1), D. A. Ennis 1), C. J. Hansen 1), N. K. Hicks 1), A. C. Hossack 1), G. J. Marklin 1), B. A. Nelson 1), R. J. Smith 1), B. S. Victor 1), J. S. Wrobel 1)

1) University of Washington, Seattle, WA 98195, USA

E-mail contact: jarboe@aa.washington.edu

Abstract. New understanding and parameters have been achieved on the Helicity Injected Torus with Steady Inductive helicity injection current drive (HIT-SI) experiment. The experiment has a one meter diameter bowtie shaped spheromak confinement region with two helicity injectors. The inductive injectors, oscillating at 5.8 kHz, are 180° segments of a small, oval-crossection RFP. Spheromaks with currents up to 38 kA and current amplification of 2 have been achieved with only 6 MW of injector power. Experiments have yielded improved current amplification and new understanding of the injector-spheromak interaction. Single injector operation shows that the two injectors have opposing, preferred spheromak current direction. An electron hyper-viscosity model is consistent with the preferred direction, with ion Doppler data, and with bolometric data. Initial experiments at 14.7 kHz injector frequency show promising results.

1. Introduction

The Helicity Injected Torus (HIT) program studies and develops helicity injection current drive for magnetic confinement. The ability to efficiently drive plasma current is an essential aspect of a wide variety of toroidal confinement approaches. Current drive by conventional means (e.g. neutral beam injection, lower hybrid waves) suffers from intrinsically low efficiency. In reactor conditions, the power coupled to the plasma through these methods needs to be as much as 1000 times greater than the minimum power to sustain the driven current against Ohmic dissipation [1,2], that is $P_{Ohm} / P_{CD} = 10^{-3}$. In contrast, helicity injection current drive has a predicted P_{Ohm} / P_{CD} of the order 0.1 for reactor conditions [3]—if developed, this two order of magnitude improvement over conventional methods could reduce the dominance of current drive cost in a reactor to insignificance. This could allow the mainline of fusion development, the tokamak, to be economically viable. If, however, the tokamak does not gain commercial acceptance, then helicity injection current drive could be all the more important to enable alternative magnetic confinement concepts that depend even more fundamentally on large amounts of efficient, externally driven current, such as spheromaks and reversed field pinches (RFPs). Good confinement has been achieved at temperatures in the kilovolt range using very little [4] or no [5,6,7,8,9,10] externally produced toroidal field. If efficient steady-state current drive with sufficient current profile control can be developed, future burning plasma experiments will not need a toroidal field coil. Elimination of this coil allows a simple vacuum vessel, further reducing complexity and cost, which may be necessary for economically competitive fusion power.[11] The HIT program is motivated by the success of Coaxial Helicity Injection (CHI) current drive on spheromaks [12] and by helicity injection current drive on RFPs [13] and tokamaks. [14] This research is to further develop and study the Steady Inductive Helicity Injection (SIHI) method that can form and sustain tokamaks, spherical tori (ST), spheromaks, and RFPs. The Helicity Injected Torus with Steady Inductive helicity injection (HIT-SI) experiment is being used to develop SIHI current drive. A description of the machine is give elsewhere. [15,16]

Some data will be compared to a "simple dynamo model" described in Reference [17] called "electron hyper-viscosity" here. One condition for electron hyper-viscosity is that the magnetic fields of the driven- and closed-flux regions must be aligned, as illustrated in

Figure 1. To locate specific regions where electron hyper-viscosity current drive may be occurring, the alignment of the fields of the injector Taylor state and spheromak Taylor state are calculated. Equilibria are calculated, assuming a spheromak λ ($\lambda \equiv \mu_0 j/B$) of 10.3 m^{-1} and injector λ of 16 m^{-1}, a typical operating value. Alignment is defined locally as $\mathbf{B}_{spheromak} \cdot \mathbf{B}_{injector}$. The results of the alignment calculation for the HIT-SI geometry are shown in Figure 1. Notice a region of positive alignment in the *left* side of the confinement volume. The calculation for the opposite phase of the injector cycle shows the region of positive alignment on the *right* side of the flux conserver. The region of alignment is therefore localized and oscillates between injector mouths with each injector half-cycle.

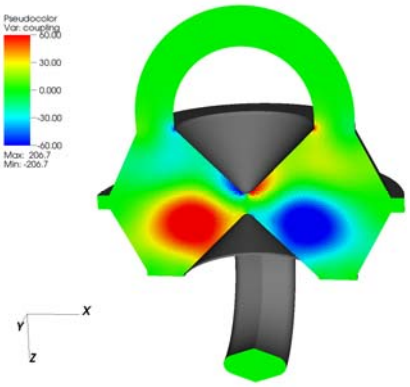

Figure 1 Calculated alignment for spheromak and injector states in HIT-SI in the plane of the injector openings. Red region on left side of flux conserver indicates alignment, and blue region on right side indicates anti-alignment.

2. Independent Injector Operation

Operations with unequal helicity injection allowed the X-injector loop voltage and flux to be increased above previous operations and resulted in new HIT-SI current records. [18] Figure 2 details the best HIT-SI shot to date (116392). Plot (a) graphs the injector loop voltages as a function of time. Shot 116392 was run with unequal helicity injection with a loop voltage amplitude on the X-injector of 450 V and a 325 V loop voltage amplitude on the Y-injector. The resulting current in each injector is shown in plot (c) and the injector currents added in quadrature [$I_{inj\_quad} = (I_{injx}^2/2 + I_{injy}^2/2)^{1/2}$] comprise plot (d). In plot (e) of Figure 2 the average total injected power is observed to be about 6 MW. Shot 116392 achieved a peak toroidal current in the confinement region of 38 kA at about 1.5 ms before flipping positive later in the discharge. The current amplification is computed by taking the ratio of the toroidal current (I_{tor}) to the injector currents added in quadrature (I_{inj_quad}) and smoothed over one injector cycle. I_{tor}/I_{inj_quad} reaches approximately 2 at about the same time the toroidal current peaks. A current amplification of 2 corresponds to a poloidal flux amplification of greater than 6.

Operations with only one injector were also successful in both forming and sustaining a spheromak equilibrium with significant toroidal current. Figure 3 is the result of running four shots with only the X-injector and four shots with only the Y-injector for the same operational settings. Figure 4 compares the toroidal currents from running only the X-injector with positive helicity plotted in red and negative helicity plotted in blue. Positive helicity is defined as having the injector current and flux in the same direction, while negative helicity has the current and flux in opposing directions. Flipping is much less common in single injector operation.

Discussion: Excellent progress has been made towards improving plasma performance and understanding of the injector-spheromak interaction. Independent injector operation has allowed for higher X-injector loop voltages, yielding a higher spheromak current of 38 kA

and a record current amplification of 2 shown in Figure 2. At this amplification the Taylor state computational analysis shows a significant amount of closed flux that does not link the injector. [19] The computation suggests the HIT-SI device is achieving regimes capable of good confinement. Additionally, operations with only one injector revealed that each injector has a preferred spheromak current direction related to the sign of the helicity and its orientation relative to the confinement volume. In Figure 3 each injector clearly demonstrates a preferred direction of generated spheromak current and furthermore they are opposed. The preferred direction of generated spheromak current results from an asymmetry of the injector-spheromak coupling combined with a mechanism beyond single-fluid MHD. The opposing current preference of each injector arises from mounting the injectors on opposite sides of the confinement volume. Figure 4 shows that the direction of preferred current is dependent of the sign of the injector helicity and changing the sign of the injected helicity switches the

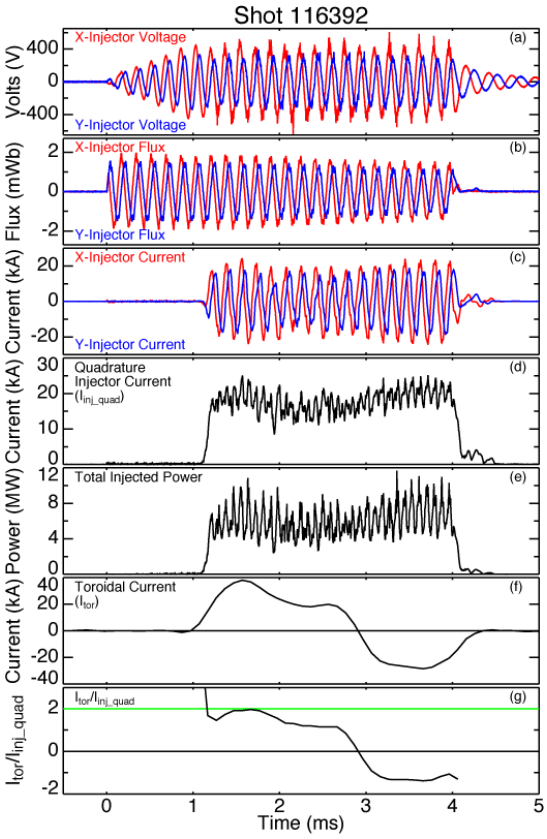

Figure 2. HIT-SI discharge with record current amplification: (a) injector loop voltages, (b) injector fluxes, (c) injector currents, (d) injector currents added in quadrature, (e) total injected power, (f) toroidal current, (g) current amplification (ratio of toroidal current to quadrature injector current boxcar smoothed over one injector cycle).

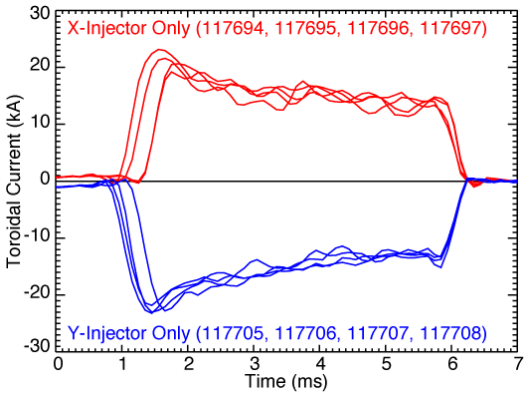

Figure 3. HIT-SI toroidal currents produced by single-injector operations.

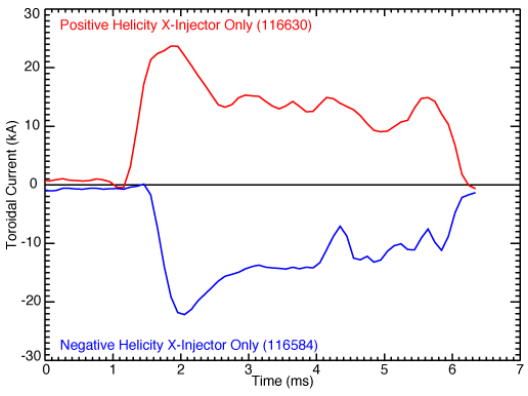

Figure 4. Resulting toroidal current in the HIT-SI during single-injector operations with positive and negative helicity injection.

the preferred direction of toroidal current. Thus, the preferred direction depends on the topology of the fields as they twist out of the injectors, which reverses when the sign of the helicity changes. While running the injector with opposite signs of helicity gives the same preferred direction it gives no helicity injection and no spheromak current. [18]

The observation of an injector having a preferred spheromak current is consistent with the electron hyper-viscosity current drive model. A single oscillating helicity injector drives electron flow into one mouth during one half-cycle and out of the same mouth during the other half-cycle. As shown previously, the location of the alignment region alternates during the injector cycle, but the phase relationship can be switched by reversing the toroidal current. For a given direction of toroidal current the alignment region will be locked in phase either with electrons flowing into the injector mouth or out of the injector mouth. It seems reasonable that the velocity gradient between the driven and closed flux regions is diminished due to the hyper-viscosity as electrons transit the spheromak volume. If the gradient is diminished before the electrons reach the region of alignment (where alignment would be phased with electrons entering the injector after transiting the volume) the current drive will not be as effective. Using this model, the preferred toroidal current direction is the sign of toroidal current which phases the *alignment region* with the electrons *exiting the injector* as observed.

The HIT-SI experiment has long observed spontaneous flipping of the direction of the toroidal current during a discharge. This becomes much less common with a single injector indicating that the toroidal current flipping is the result of the opposing directions of preferred current for each injector. Apparently, during the dual injector operation the two injectors trade dominance back and forth over the direction of the toroidal current.

3. Bolometer data

As shown in Figure 5 a bolometer observes a region in front of one of the injector mouths on HIT-SI. A peak in radiated power is observed at every injector half-cycle because the bolometer views the injector opening. In the first few cycles, the radiation peak height alternates. In Figure 6, higher peaks are indicated with dashed lines drawn through them.

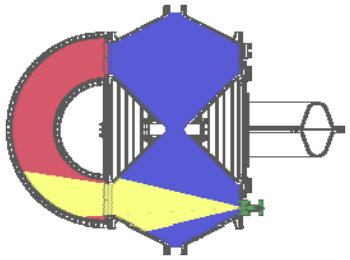

Figure 5 Cutaway of HIT-SI with both the active injector (left) and the "bowtie" spheromak region (middle). The bolometer is located in the lower right with the viewing cone highlighted.

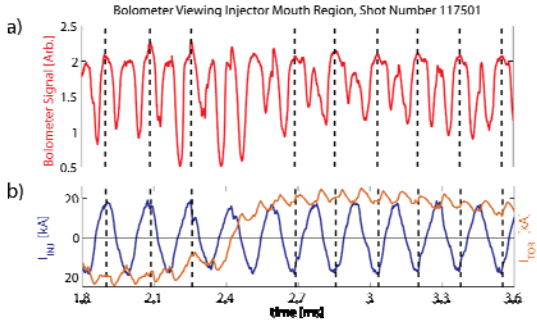

Figure 6 a) Bolometer amplitude (radiated power) during a portion of the discharge. The bolometer has a 20 μs rise time. b) Measured injector current (blue trace) and total toroidal current in the confinement volume (brown trace).

Later in the discharge, the spheromak toroidal current reverses direction. Dashed lines are once again drawn through the higher peaks in radiation. Notice the relative phasing of the peak bolometry data to injector current has changed.

Discussion: That the bolometer signal peaks every half-cycle is not surprising since the power to the injector has the same signature. However, the peaks are not equal and the phasing of the higher peak with respect to injector current changes when the spheromak flips.

This behavior must be caused by an asymmetry in the interaction between the injector and the spheromak. One possible asymmetry is the alignment shown in Figure 1. The higher radiation appears when the bolometer is viewing positive alignment. This is expected from the electron hyper-viscosity model because alignment is required for the cross field coupling. Higher coupling will cause more power to be deposited locally, some of which is radiated to the bolometer. The alignment calculation also shows that reversing the direction of spheromak current *also* changes the region where alignment occurs. The data reflect this because the phase of increased radiation changes when the spheromak flips. For the shot presented in Figure 6, the spheromak current flipped to its preferred direction and the alignment calculations indicate that the alignment region became phased with electrons exiting the injector.

4. Ion Doppler Spectroscopy

An Ion Doppler Spectrometer (IDS) measures the velocity of the bulk ion species at the He II wavelength of 468.57 nm. The configuration on the machine is similar to the bolometer (see Figure 5) except that the viewing cone is a 25 mm diameter column extending into the injector mouth. IDS velocity is displayed in Figure 7a, along with the injector loop voltage in Figure 7b. Dashed lines are drawn through the peaks in ion velocity; they align with the phase of injector voltage such that the injector-produced E-field is in the direction of the ion velocity. Both are out of the injector at the times of the dashed lines.

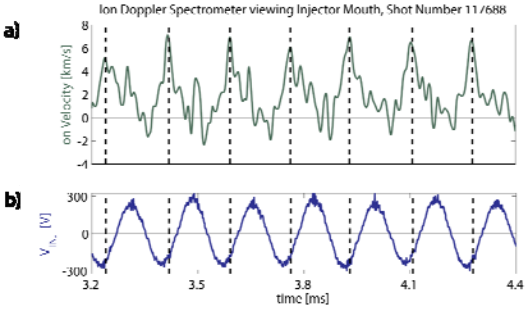

Figure 7 a) IDS velocity trace normal to the injector mouth with dashed lines drawn through maxima and injector loop voltage trace (b).

Discussion: The large 5.8 kHz component of the ion Doppler spectroscopy signal is not consistent with resistive MHD and is consistent with electron hyper-viscosity. Flow out of the injector is expected because of the higher pressure in the injector and the flow might be higher at peaks in heating ($\propto I^2$) yielding a DC flow with an 11.6 kHz ripple, not the 5.8 kHz observed. The bulk ion velocity fluctuates by more than 6 km/s, orders of magnitude above the MHD classical ion drift velocity contribution to the injector current of ~30 m/s. The phasing and the frequency of the ion velocity agree with the electron hyper-viscosity model. The anti-current drive in this externally driven region puts an additional force on the electrons necessitating an E-field larger than needed to just overcome resistive drag. The large E-field also acts on the ions and accelerates them because it is larger than needed to overcome the equal and opposite resistive drag on the ions and the ions do not experience the anti-current drive. They are accelerated in the direction of the current as observed.

5. High Frequency Operation

The effect of higher-frequency operations on generating and sustaining a spheromak has been tested on HIT-SI machine by increasing the injector frequency to 14.7 kHz from previous operations at 5.8 kHz. Moving from 5.8 kHz to 14.7 kHz changed the relationship between the injector drive and the Alfvén time of the machine. The toroidal transit time of an Alfvén wave around the major axis is ~24 μs, compared to the inverse angular frequencies of the injectors of 27 μs at 5.8 kHz and 11 μs at 14.7 kHz. Figure 8 shows data for shots at 5.8 kHz (#117399) and 14.7 kHz (#118834) with similar quadrature injector voltages. Both injectors

for the 14.7 kHz shot have similar power input ('equal-injector operations'), while one of the injectors for the 5.8 kHz shot inputs about twice as much power as the other injector. For 5.8 kHz operation the three-turn 2.4 μH primary of the voltage circuit is placed in parallel with a 680 μF capacitor. The pair is driven by a pulse-width-modulated power supply in series with a 2 μH inductor, forming a tank circuit. For 14.7 kHz operation the 680 μF capacitor is replaced with a 100 μF capacitor. The series inductance is adjusted for tuning. For 5.8 kHz operation the eight turn, 1.9 μH flux coil is driven directly by pulse-width-modulated power supplies with 50,000 pulses per second controlling the flux. For 14.7 kHz operation, feedback control of the flux during the cycle was no longer possible and a triangular wave of about 1.2 mWb is achieved by simply switching the power supplies between plus and minus at the appropriate times.

Figure 9 and Figure 10 show the equilibrium internal magnetic fields and the Taylor state values for the two different injector frequencies. The Taylor state [13,20] is scaled using the toroidal plasma current calculated from the external flux loops, shown in part c) of each figure. Thus, the plot of the Taylor state is completely independent of the internal magnetic field measurements. Density verses time on HIT-SI typically shows an equilibrium density with fluctuations in the density at the frequency of the injectors. During 5.8 kHz operations the density fluctuations at the injector frequency are enough to double the density. This can be seen in the dark trace of Figure 11a, where the line-averaged density increases to 8 x 10^{19} m^{-3} from an average density of 3 - 4 x 10^{19} m^{-3}. The fluctuations in density at the injector frequency are smaller and more uniform during 14.7 kHz operations as seen in Figure 11a.

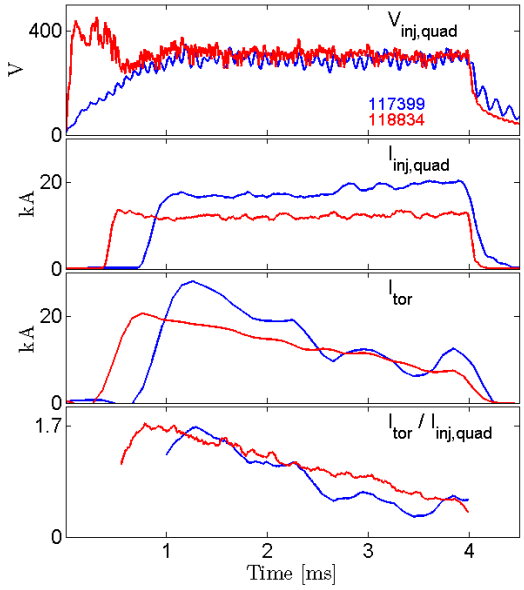

Figure 8. Comparison between 5.8 kHz (blue) and 14.7 kHz (red) operations: a) Quadrature injector voltage, b) Quadrature injector current, c) Toroidal plasma current, and d) Current amplification

Discussion: Fueling rates that produce the highest toroidal plasma currents are lower for 14.7 kHz operations than 5.8 kHz. Thus plasma discharges at 14.7 kHz have a lower average density than plasma discharges at 5.8 kHz. Operating HIT-SI with a lower fueling rate has increased the ratio of plasma current to electron density. Plasmas operating below the Greenwald current limit tend to be radiation dominated [21,22]. Radiation losses are a concern on HIT-SI and increases in the ratio of plasma current to electron density are seen as a sign of improved performance. Figure 11b shows the ratio of plasma current density (calculated by averaging the current measured by the external flux loops over a poloidal cross section) to electron density (averaged over an injector cycle). This ratio is consistently higher for the 14.7 kHz operations. In Figure 8 the current amplification, gives a measure of the effectiveness in coupling injected helicity to the spheromak. With similar loop voltages the 5.8 kHz shot has a higher injector and peak plasma current, but the plasma

current rapidly decreases in the second half of the shot. Despite not having as high of an initial plasma current, the ratio of plasma to injector current at 14.7 kHz compares favorably to 5.8 kHz. The current amplification of 1.7 is higher than ever achieved with equal injector

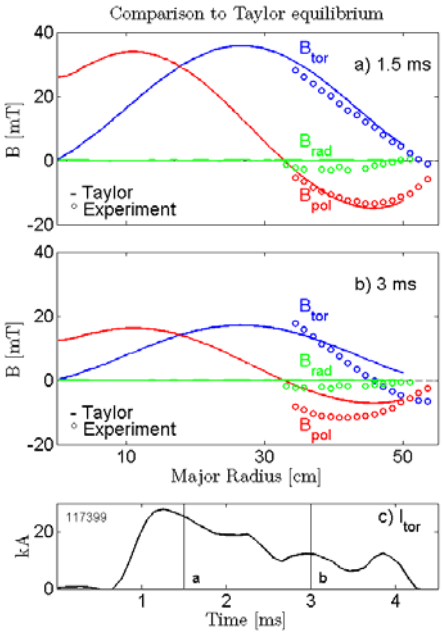

Figure 9. Comparison of measured internal magnetic fields to Taylor state for a 5.8 kHz shot: a) Magnetic fields match Taylor state at 1.5 ms, b) Magnetic fields no longer match Taylor state at 3 ms, and c) Toroidal plasma current as measured by the external flux loops. Shot#117399

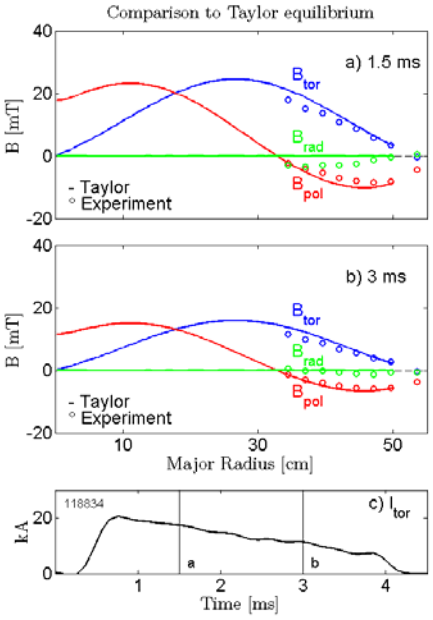

Figure 10. Comparison of measured internal magnetic fields to Taylor state for a 14.7 kHz shot: a) and b) Magnetic fields match Taylor state at 1.5 and 3 ms respectively and c) Toroidal plasma current as measured by the external flux loops. Shot#118834

operations at 5.8 kHz. Additionally, the plasma current driven at 14.7 kHz shows a slow, smooth decay throughout the shot, without the rapid drop seen at 5.8 kHz.

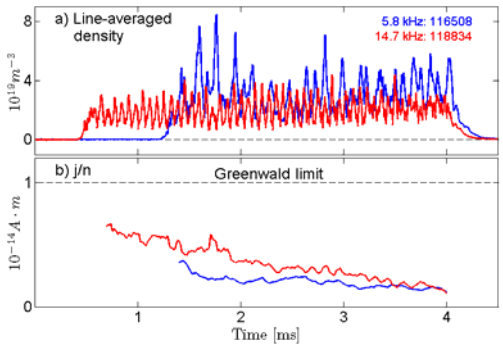

Figure 11. a) Comparison of the line-averaged density at 5.8 and 14.7 kHz b) Ratio of current density to electron density (averaged over an injector cycle) is increased for 14.7 kHz operations

During the first 2.5 ms of the 5.8 kHz shot of Figure 9 the measured magnetic field matches the Taylor state. Part a) shows the comparison at 1.5 ms. At about 2.5 ms the toroidal plasma current has a sharp drop and from this moment on the Taylor state is no longer an accurate predictor of the internal fields. Part b) shows the deviation of the internal magnetic field from the Taylor state at 3 ms. Similar to 5.8 kHz operations, initially the Taylor state matches the internal magnetic field profile for 14.7 kHz operations as can be seen in Figure 10a. Typical of other shots at 14.7 kHz, the shot shown in Figure 10 shows a slow decay in toroidal plasma current with the Taylor state matching the internal magnetic field profile for a longer duration of time as seen in Figure

10b. Lower density, which is required to achieve the Greenwald limit, is achieved at higher frequency. Smaller fluctuations are also achieved at higher frequency. The higher current amplification, lower and smoother density, and smoother spheromak current all indicate that higher frequency will give better performance.

6. Conclusion

HIT-SI operation has been quite successful with spheromak currents up to 38 kA, twice the injector current amplitude, with only 6 MW of injector power. For the same sign of helicity, a requirement for spheromak formation, the injectors have opposite preferred directions because they are mounted on opposite sides of the spheromak volume. This leads to spheromak flipping during the shot, apparently from the alternating of dominance during the discharge. The preferred direction and key features of the bolometry and IDS data are explained by the electron hyper-viscosity model but more work is needed to fully confirm the model. Operations at higher injector frequency have shown improved plasma performance and operation. Initial results at higher injector frequency have demonstrated improved current amplification for equal-injector operations, sustained magnetic profiles similar to the predicted Taylor state, and an improved ratio of current to electron density with lower density fluctuations and less fueling required.

7. Acknowledgements

The authors would like to thank John Rogers and George Andexler for their advice and technical assistance and Professor Nagata of the University of Hyogo for the continued loan of the IDS instrument.

---

[1] Fisch N., Rev. Mod. Phys. **59**, 175 (1987).
[2] Boozer A. H., Phys. Fluids **31**, 591 (1988).
[3] Jarboe T. R., Fusion Technology **15**, 7 (1989).
[4] Sarff, J. S. *et al*., Nuclear Fusion, **43**, pp. 1684-1692 (2003).
[5] Fowler T. K. *et al.*, Comments Plasma Phys. Controlled Fusion, **16**, 91 (1994).
[6] Hooper E. B. *et al*., Fusion Technology **49**, 191 (1996).
[7] Fowler T. K. *et al*., Fusion Technology **49**, 206 (1996).
[8] Hooper E. B. *et al.*, IAEA 1998.
[9] B. Hudson *et al.,* Phys. Plasmas **15**, 056112 (2008)
[10] Jarboe T. R. *et al.,* Phys. Fluids B, **2**, 1342 (1990).
[11] Hagenson R. L. and Krakowski R. A., Fusion Technol. **8**, 1606 (1985).
[12] Jarboe T. R., Plasma Phys. Control. Fusion **36**, 945 (1994).
[13] Taylor J. B., Rev. Mod. Phys. **58**, 741 (1986).
[14] Ono M. *et al.*, Phys. Rev. Lett. **59**, 2165 (1987).
[15] Sieck P. E. *et al*., IEEE Trans. Plasma Sci., **33**, 723 (2005).
[16] Sieck P. E. *et al*., Nuc. Fusion, **46**, 254, (2006).
[17] Jarboe T. R., Plasma Phys. Control. Fusion **52** (2010) 045001 (9pp)
[18] Ennis D.A. *et al.*, Nucl. Fusion, **50,** 072001 (2010).
[19] Jarboe T. R. *et al*., Phys. Rev. Lett., **97,** 115003 (2006).
[20] O'Neill R. G. *et al.,* Phys. Plasmas **14**, 112304 (2007).
[21] M. Greenwald et al., Nucl. Fusion **28**, 2199 (1988).
[22] Jarboe T. R., Phys. Plasmas **12**, 058103 (2005).